Holographic detection of a tooth structure deformation after dental filling polymerization

Dejan Pantelić
Institute of Physics
Pregrevica 118
11080 Zemun, Belgrade
Serbia
E-mail: pantelic@phy.bg.ac.yu

Larisa Blažić
University of Novi Sad
Faculty of Medicine
Dental Clinic
Hajduk Veljkova 12
21000 Novi Sad
Serbia

Svetlana Savić-Šević
Bratimir Panić
Institute of Physics
Pregrevica 118
11080 Zemun, Belgrade
Serbia

Abstract. An experimental technique to reveal the effects of dental polymer contraction is established to choose the most appropriate polymerization technique. Tooth deformation following a dental filling polymerization is analyzed using double-exposure holographic interferometry. A caries-free, extracted human molar is mounted in dental gypsum and different cavity preparations and fillings are made on the same tooth. Dental composite fillings are polymerized by an LED light source especially designed for this purpose. Holographic interferograms are made for occlusal (class I), occlusomesial (class II), and mesioocclusodistal (class II MOD) cavities and fillings. Maximum intercuspal deformation ranges from 2 μm for the class I cavity to 14 μm for the MOD class cavity. A finite element method (FEM) is used to calculate von Mises stress on a simplified tooth model, based on experimental results. The stress varies between 50 and 100 MPa, depending on the cavity type. [DOI: 10.1117/1.2714056]

Keywords: holography; interferometry; biomechanics; dental composites.

Paper 06046RR received Mar. 3, 2006; revised manuscript received Nov. 22, 2006; accepted for publication Nov. 27, 2006; published online Mar. 12, 2007.

1 Introduction

Polymerization shrinkage of dental composites is still a cause of serious clinical problems such as loss of bonding between composite and a tooth, or microfractures of a tooth tissue, both resulting in premature dental filling failure.[1] In addition, stress caused by polymerization contraction may also cause postoperative sensitivity.[2] It is difficult to directly measure stress induced by dental composite contraction, as it is distributed inside the tooth. Instead, the resulting deformation of a tooth surface is measured and the stress is estimated.

The current research is performed in several directions. One deals with linear and volumetric contraction of pure composite layers (outside the dental cavity).[3–7] The second, clinically more relevant approach focuses on measuring tooth deformation induced by the composite inside the dental cavity. Changes in tooth structure and the resulting cuspal deflection[8–11] due to polymerization shrinkage are detected by several measurement techniques: microscopy,[12] strain gauges,[13] interferometry,[14] and photoelasticity.[15,16]

The third, computational, approach analyzes both deformation and the resulting stress, using the finite element method[17–20] (FEM). This is essentially a computer simulation that gives detailed information about shrinkage stresses, but does not take into consideration specific differences in human teeth which vary considerably in their coronal morphology and mechanical properties.[21] Therefore, the same results for numerical and experimental studies cannot be expected, because the total shrinkage and the resulting stress are dependent on the cavity shape, tooth tissue structure, and the properties of the composite material, bonding system, and polymerization process.

As can be seen, a method connecting experimental measurements of dental deformation with numerical calculation of internal stress is necessary. First, complete deformation field should be measured, and then the FEM should be applied to determine stress inside the tooth.

Holography offers a solution to the problem of the deformation field measurement. In particular, laser interferometry by holography is a nondestructive method for measurement of mechanical deformations of different structures and materials. Deformation is seen as a system of dark and bright fringes superposed on the 3-D holographic image. The fringes are maps of the investigated structure deformation and represent an extremely sensitive picture of displacements caused by mechanical stress.

Holographic interferometry was used previously to investigate various dental tissues or dental implants.[22–26] To our knowledge, this paper is the first holographic study of a complete tooth deformation field induced by dental composite shrinkage. The holographic interferometry method was used (*in vitro*) to determine the total deformation at any point of the tooth surface. Based on experimental data, the resulting stress was calculated using the FEM.

2 Method

Caries-free extracted human third molars were used. They were kept in a saline solution at 4°C to preserve their biological and mechanical properties. Just before measurement, the

Address all correspondence to Dejan Pantelic, Lasers and Optoelectronics, Institute of Physics, Pregrevica 118, 11080 Zemun, Belgrade, Serbia; Tel: 381 11 3160793; Fax: 381 11 3162190; E-mail: pantelic@phy.bg.ac.yu

1083-3668/2007/12(2)/024026/7/$25.00 © 2007 SPIE

Fig. 1 Tooth mounted in dental gypsum in an inclined position.

tooth was mounted in an inclined position using dental gypsum, in a manner shown in Fig. 1. After drying, a good mechanical contact between the tooth and gypsum was obtained, enabling stability during holographic measurements.

Standard cavity preparations and restorations were made (class I, class II, and class II MOD) and the configuration is shown schematically in Figs. 2(a)–2(c). They were cut using a diamond coated burr attached to the water-cooled air turbine. Each cavity was prepared for dental composite placement by the "Prompt L Pop" adhesive system according to the manufacturer's (3M ESPE, Seefeld, Germany) instruction. Consequently, the cavities were filled in one increment (bulk technique) with a commercially available dental composite resin "Filtek Z 250" (3M ESPE, Seefeld, Germany).

Dental composite resin was polymerized by an LED light source, specially designed for research purposes. LED diodes (42 of them in total, with 10 mW of optical output power, each) were mounted on the hemispherical holder [Figs. 3(a) and 3(b)]. The light source produced an evenly illuminated circular spot (more than 1 cm in diameter) at the center of a sphere where the tooth was placed, illuminated, and a dental filling was polymerized. This enabled contactless operation, in contrast to commercial devices, where the LED lamp tip should be in complete contact with dental polymer.

Operation without contact is important in holographic research, where extreme mechanical stability is required. Additionally, possible heat transfer from the LED to the tooth is negligible, because LEDs dissipate only a small amount of heat and the tooth is 30 mm from the lamp.

The tooth surface must be painted to improve fringe visibility in the resulting holographic interferogram.[26,27] A paint layer must be thin, but opaque to laser radiation and capable of drying fast. A silver marker [PX-20(L) produced by Mitsubishi Pencil Co. Ltd.] served this purpose perfectly.

Double-exposure holograms were produced using a simple split beam setup (Fig. 4) with 10-mW power, 632.8-nm wavelength HeNe laser. The LED lamp was positioned above the tooth to induce polymerization. The first holographic exposure (of 5-s duration) was made before polymerization. The LED lamp was turned on for the time period necessary to induce complete polymerization. Subsequently, the LED source was turned off and the second holographic exposure (5 s) was made. Therefore, two holographic images were recorded on the same holographic photosensitive material (silver halide glass plate, Agfa 8E75HD).

Following the standard chemical processing (development, fixing, bleaching, and drying), the hologram plate was returned to its original position and prepared for reconstruction and analysis. On reconstruction two coherent images were seen—one corresponding to the undeformed and the other to the deformed state of the tooth. Interference of these two

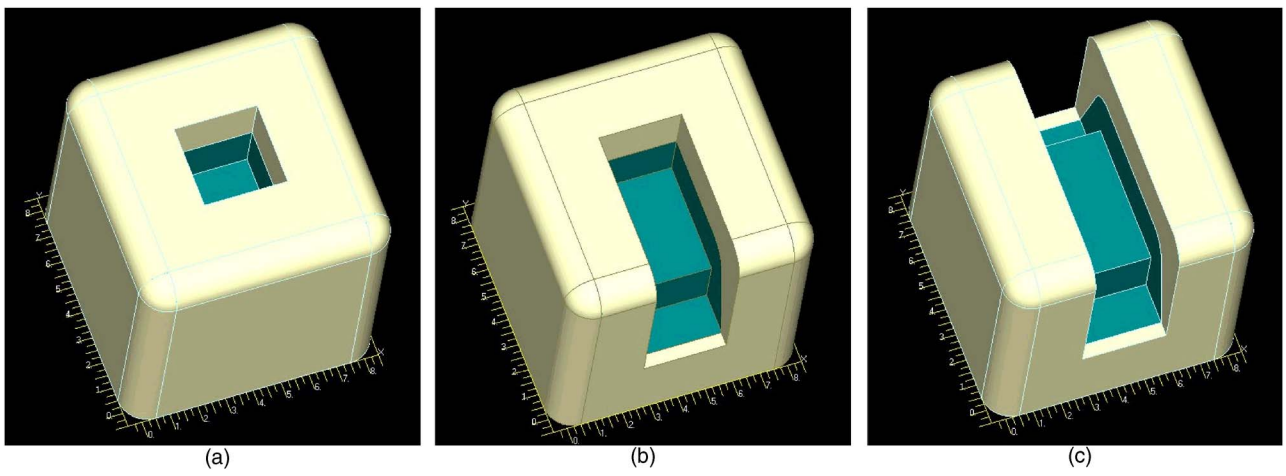

Fig. 2 Standard dental cavity configurations: (a) class I, (b) class II, and (c) class II MOD.

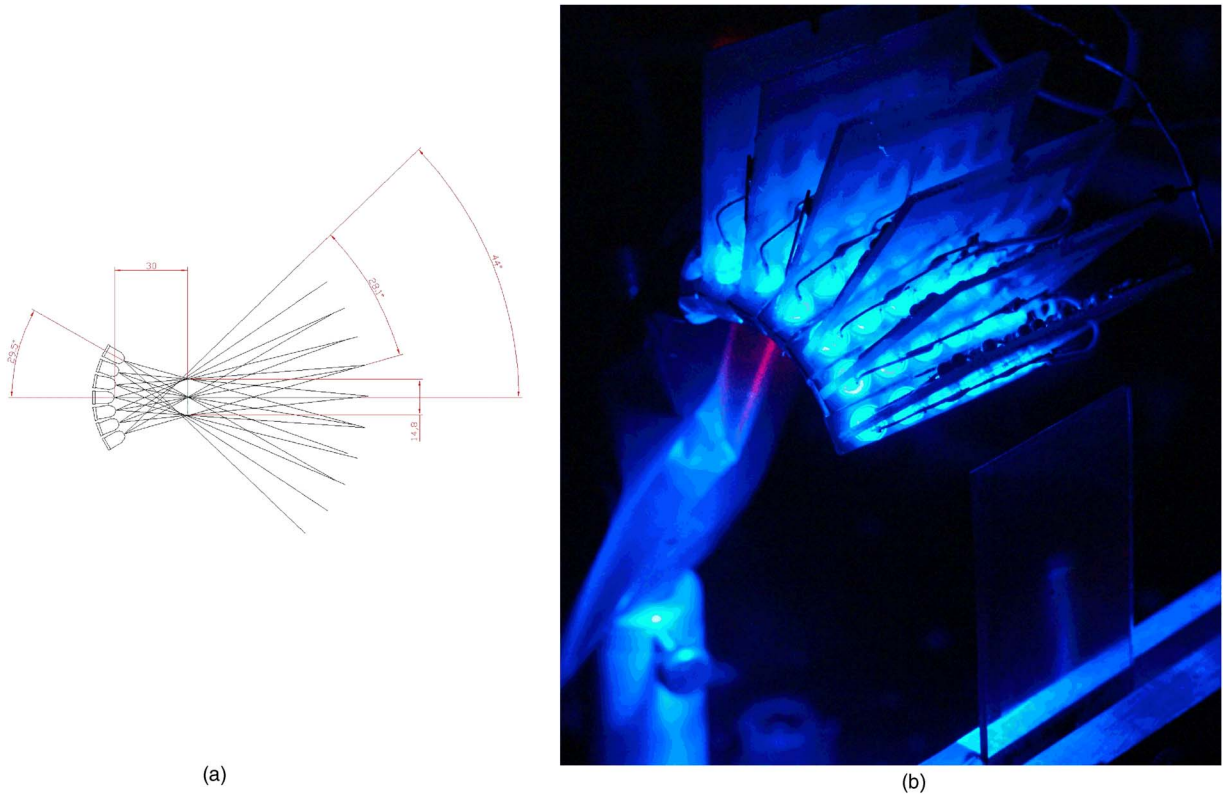

Fig. 3 LED lamp used during experiments produces even illumination on a circle with more than 1 cm diameter: (a) technical drawing with dimensions in millimeters and (b) photograph of an LED lamp.

images produces a series of dark and bright fringes—an interferogram.

The holographic interferogram was made first for the occlusal cavity (class I), and then the same procedure was repeated for the occlusomesial cavity (class II) and the mesioocclusodistal cavity (class II MOD). All cavities were made in the same tooth specimen by gradually increasing the cavity dimension from class I to class II MOD type.

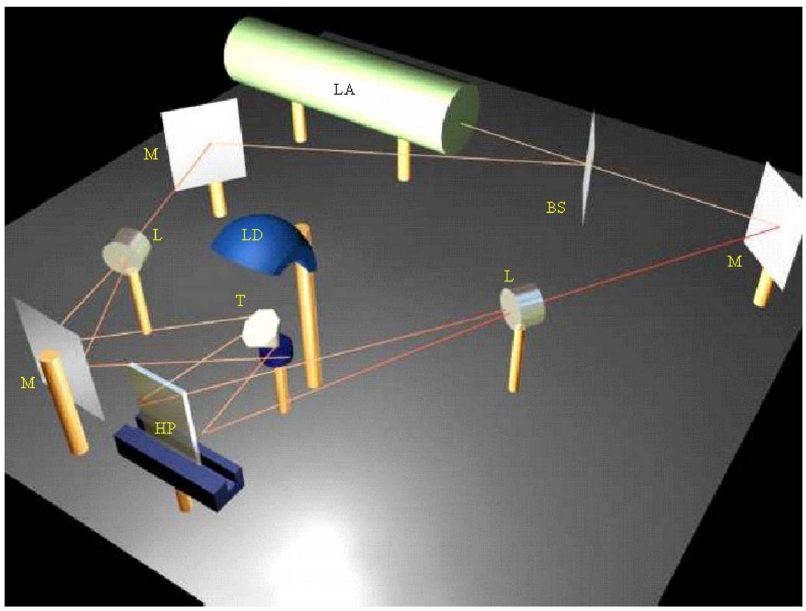

Fig. 4 Holographic interferometry setup: LA, laser; BS, beamsplitter; M, mirror; L, diverging lens (pinhole filter); HP, holographic plate; T, tooth; LD, LED lamp.

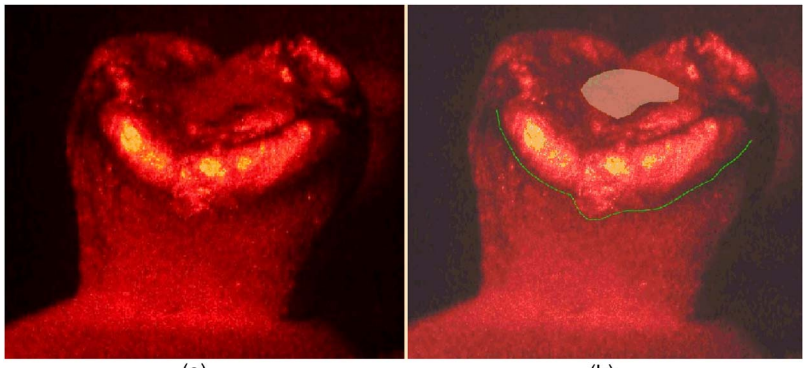

Fig. 5 Tooth hologram reconstruction of (a) class I cavity and (b) class I cavity with contour lines drawn (numbers designate deformation in micrometers).

3 Results of Holographic Measurements

As a general conclusion, it was found that a larger volume of composite material (due to a larger cavity) induced more strain. Photographs show a series of interferograms obtained for occlusal cavity [class I, Figs. 5(a) and 5(b)], occlusomesial cavity [class II, Figs. 6(a) and 6(b)], and mesioocclusodistal cavity (class II MOD, Figs. 7(a) and 7(b)). Figures 5(a), 6(a), and 7(a) are the original photographs, while in Figs. 5(b), 6(b), and 7(b) dark fringes are emphasized by lines with numbers indicating the corresponding deformation in micrometers (i.e., deformation is constant along each line or fringe).

Obviously, number of fringes increases with an increased cavity size. An occlusal cavity produced only one, barely visible, fringe at the tooth cusp [Figs. 5(a) and 5(b)]. Fringe number increases to 7 for the occlusomesial cavity [Figs. 6(a) and 6(b)], and for mesioocclusodistal cavity [Figs. 7(a) and 7(b)], 12 fringes are visible. Knowing the wavelength of the laser radiation (633 nm), it was concluded that maximum deflections range from, approximately, 1 (class I cavity) to 7 μm (class II MOD cavity).

In our experiment, we could see only one side of a tooth, while the other was completely invisible. It can be assumed that roughly the same deformation was produced on the hidden side, since a tooth is almost symmetrical with respect to the mesiodistal line, and cavities were also intentionally drilled symmetrically (see Fig. 1). Therefore, the resulting intercuspal movement ranges from 2 to 14 μm (double of what was observed on one side of the tooth).

4 Mechanical Model and Finite Element Calculation of Mechanical Stress

The FEM is a powerful tool in dentistry. However, its results should be treated more as an estimate, rather than an exact

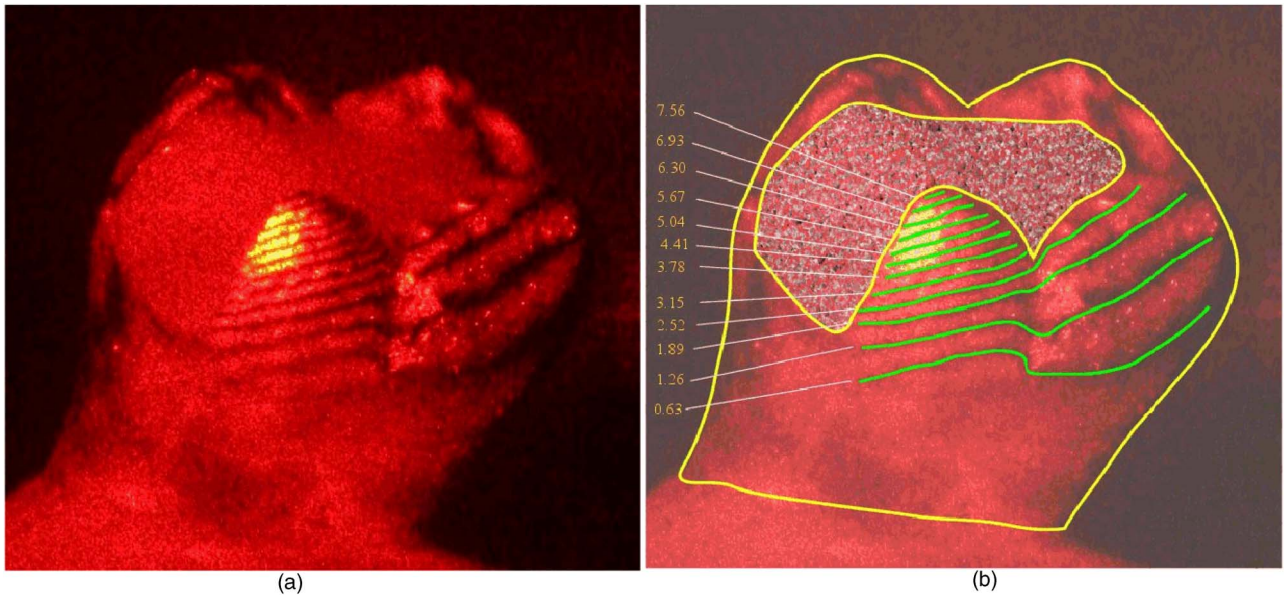

Fig. 6 Tooth hologram reconstruction of (a) class II cavity and (b) class II cavity with contour lines drawn (numbers designate deformation in micrometers).

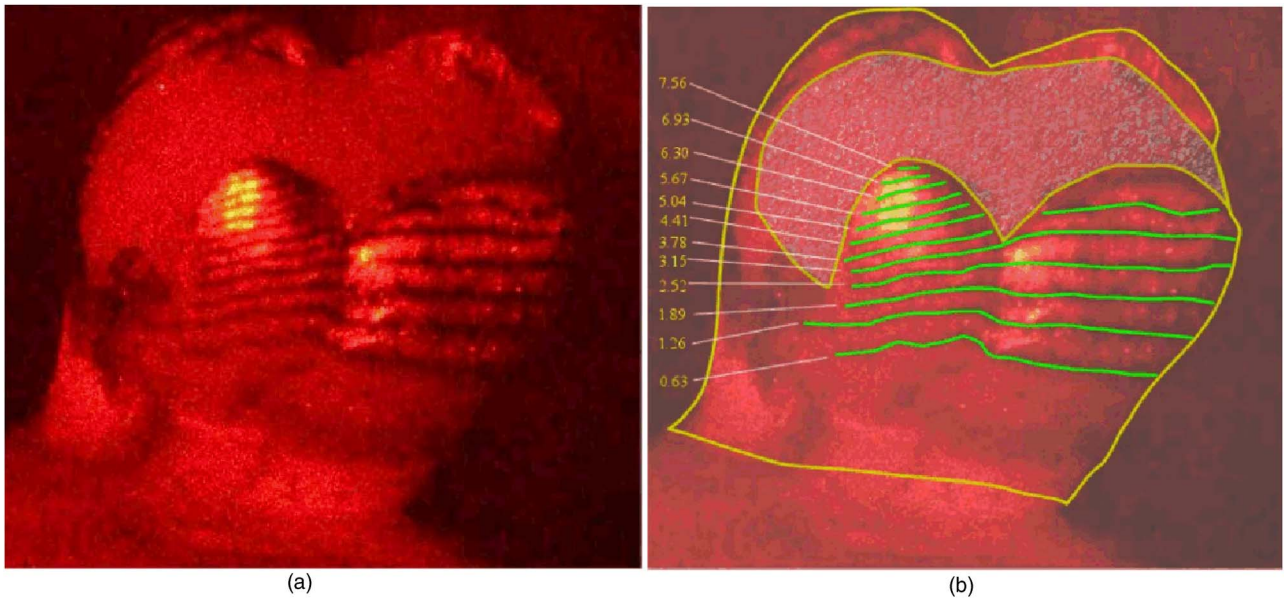

Fig. 7 Tooth hologram reconstruction of (a) class II MOD cavity and (b) class II MOD cavity with contour lines drawn (numbers designate deformation in micrometers).

picture of the actual stress distribution inside the dental tissue. This is due to natural variability in properties of teeth, differences in characteristics of dental polymers, and because of approximations made during modeling and calculation.

Teeth were previously modeled in many ways, and stress and strain were calculated. Two-dimensional (2-D) and 3-D models were constructed by approximating a tooth with a cylinder[28] or a parallelepiped.[17] More realistic mechanical models were obtained by computerized tomography[29] (CT) or laser scanning of a real tooth.[30]

In general, results obtained by approximating a tooth[17,28] are quite similar to more comprehensive models.[18,30] Stress distributions are comparable and numerical values of maximum von Mises stress are roughly the same.

Therefore, a simplified tooth model was developed, similar to one described in Ref. 17. The tooth was approximated, as shown in Fig. 8, with a cube made of enamel [Young's modulus 60 GPa, Poisson's ratio 0.3 (Ref. 17)], with its interior composed of dentin [Young's modulus 15 GPa, Poisson's ratio 0.31 (Ref. 17)]. It was assumed that materials are linear and isotropic, as usually accepted in the literature.[30] Interfaces between dental filling, dentine, and enamel were treated as rigid. Mesh was refined up to 19,089 nodes, and 11,526 10-point tetrahedral elements to test the model for convergence.

The bottom surface of a parallelepiped was rigidly constrained, so that the model actually approximates a tooth cusp. This was reasonable since the stress is only slightly transferred to the tooth root, as shown in FEM study of Ausiello et al.[30]

Different types of cavities were made in a digital model [Figs. 2(a)–2(c)] and analyzed using the FEM. It is known that dental composite contracts volumetrically and isotropically. We have, therefore, assumed that the composite exerts constant pressure on the cavity walls.

The exact value of the pressure exerted by the composite on the cavity walls is not known. Therefore, the pressure on the cavity sides was varied until the deformation of the model matched that observed experimentally. This is an iterative procedure that starts with an arbitrarily chosen value of the cavity internal pressure. A resulting deformation field is calculated using the FEM and deflections are compared to the holographic interferogram. If the difference between the model and experiment is unacceptably high, internal pressure is changed and model recalculated. The procedure is repeated until experiment and theory are within the measurement uncertainty (of the order of one interference fringe—0.633 μm). Luckily, this is achieved in 5 to 10 iterations, making the procedure not too time consuming. The resulting deformation patterns, shown in Figs. 9(a)–9(c), compare well with experi-

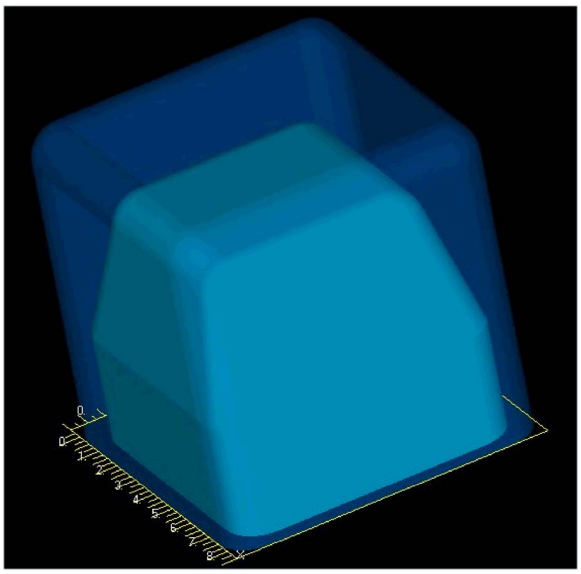

Fig. 8 Simplified mechanical model of a tooth.

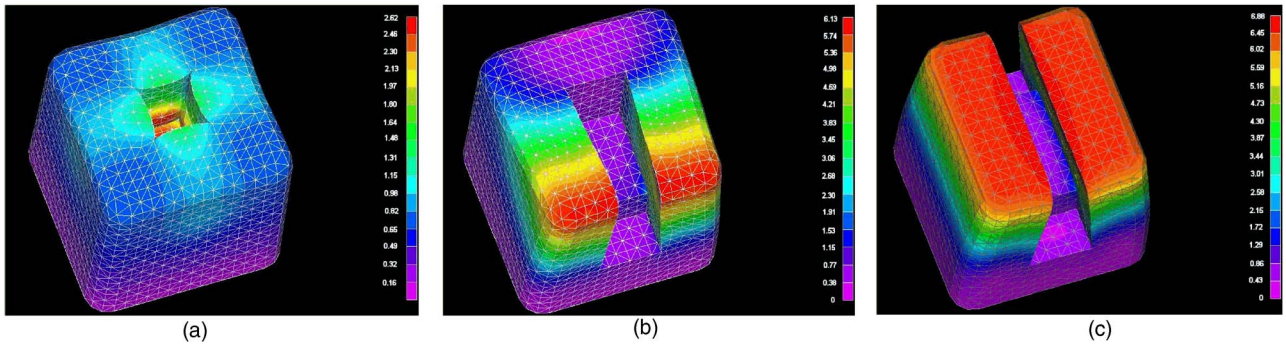

Fig. 9 Tooth deformation as calculated by the FEM for the cases of (a) a class I cavity, (b) a class II cavity, and (c) a class II MOD cavity. Colored contours represent deformation in micrometers (as shown in the bar on the right side of the figure).

mentally recorded deformation fields [Figs. 5–7]. Related von Mises internal stress was calculated for each cavity type [Figs. 10(a)–10(c)].

We found that the maximum von Mises internal stress varies from 50 to 100 MPa, depending on the cavity type. It was the highest in the case of class I cavity, lower in the class II type, and the lowest in the MOD cavity. Note that the preceding calculations produce only "the order of magnitude" of stress. A more exact model would require tomographic tooth analysis.

The stress obtained in our research (50 to 100 MPa), agrees with literature data.[18,31] It reaches a rather high value, if compared to mechanical strength of dentin (40 to 140 MPa, see Refs. 32 and 33) and enamel (11.5 to 95 MPa, see Refs. 32 and 34). Therefore, we can conclude that there is a real danger of damaging dental tissues. Luckily, areas of high stress are localized to cavity edges [as can be seen in Figs. 10(a)–10(c)] and may cause confined effects (microcracking, composite debonding).

5 Discussion and Conclusions

Tooth tissues have microscopic features (the so-called prisms in enamel, with approximately 5 μm diameter and 2 to 4 μm microtubules in dentin) that strongly scatter and diffract light, as shown in many research papers.[35–38] During polymerization, a tooth is subjected to deformation of up to 14 μm (as we found holographically), which is large compared to dimensions of dental microstructures. This necessarily induces major changes in the profile of a back-scattered light wave.

In double-exposure holography, two significantly different wavefronts produce interference fringes with very high density—well above the resolving power of a detection system (camera or eye). This is exactly what we have in our experiment: wavefronts before and after polymerization are quite different. The final outcome is that fringes become practically invisible.

To verify the assumption that polymerization contraction induces internal changes of dentin and enamel, we made double-exposure tooth interferogram without polymerization. Between exposures, the tooth was deliberately translated (without deformation). As a result, fringes with high-contrast were obtained after processing. Thus, we can conclude that if a tissue is not deformed, high-contrast fringes are obtained. If it is deformed, the interference pattern vanishes due to internal distortion of dental microstructures.

The purpose of this paper was to introduce holography as a measurement method for the tooth deformation field, due to composite polymerization contraction. It was found that the number and shape of the resulting interference fringes depend on the particular tooth and dental cavity design. In general, total deformation was the smallest at the tooth root and the largest at its cusp. We found that total intercuspal displacement is between 2 and 14 μm, which is comparable to a numerical study[18] where the calculated deformation was 10 to

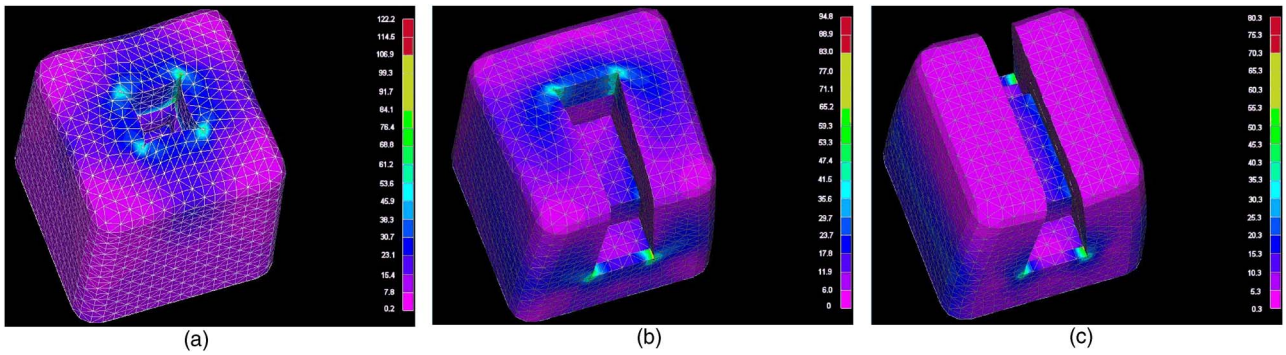

Fig. 10 Von Mises stress distribution in a tooth with a (a) class I cavity, (b) class II cavity, and (c) class II MOD cavity. Colored contours represent stress in megapascals (as shown in the bar on the right side of the figure).

20 μm. The strain due to setting of composite restoration was quantified previously by measuring cuspal movement,[12,36,39] with similar experimental results.

The resulting stress was calculated using the FEM applied to the simplified tooth model. Correspondence with measurements was established, and the resulting maximum stress was estimated between 50 and 100 MPa. To achieve more exact picture of dental stress, tomographic methods should be used.

Finally, holographic interferometry has indirectly indicated that there are alterations in internal structure of dental tissues caused by polymerization contraction of composite material. This was verified by the almost total absence of an interference pattern in the case of an unpainted tooth surface.

Acknowledgments

This work was supported by the Serbian Ministry of Science and Environmental Protection under the Contract No. 141003.

References

1. D. Tantbirojn, A. Versluis, M. R. Pintado, R. DeLong, and W. H. Douglas, "Tooth deformation patterns in molars after composite restoration," *Dent. Mater.* **20**, 535–542 (2004).
2. N. J. M. Opdam, F. J. M. Roeters, A. J. Feilzer, and E. H. Verdonschot, "Marginal integrity and postoperative sensitivity in class 2 resin composite restoration in vivo," *J. Dent.* **26**, 555–562 (1998).
3. C. Alvarez-Gayosso, F. Barcelo-Santana, J. Guerrero-Ibarra, G. Saez-Espınola, and M. A. Canseco-Martınez, "Calculation of contraction rates due to shrinkage in light-cured composites," *Dent. Mater.* **20**, 228–235 (2004).
4. R. L. Sakaguchi, B. D. Wiltbank, and N. C. Shah, "Critical configuration analysis of four methods or measuring polymerization shrinkage strain of composites," *Dent. Mater.* **20**, 388–396 (2004).
5. J. H. Lai and A. E. Johnson, "Measuring polymerization shrinkage of photo-activated restorative materials by a water-filled dilatometer," *Dent. Mater.* **16**, 172–176 (1993).
6. C. L. Davidson, A. J. De Gee, and A. J. Feilzer, "True linear polymerization shrinkage of unfilled resin and composites determined with a linometer," *Dent. Mater.* **9**, 11–14 (1993).
7. E. A. Fogleman, M. T. Kelly, and W. T. Grubbs, "Laser interferometric method for measuring linear polymerization shrinkage in light cured dental restoratives," *Dent. Mater.* **18**, 324–330 (2002).
8. R. H. Kuijs, W. M. M. Fennis, C. M. Kreulen, M. Barink, and N. Verdonschof, "Does layering minimize shrinkage stresses in composite restorations?" *J. Dent. Res.* **82**, 967–971 (2003).
9. N. Martin, N. M. Jedynakiewicz, and D. F. Williams, "Cuspal deflection during polymerization on composite lutes of ceramic inlays," *J. Dent.* **27**, 29–36 (1999).
10. B. E. Causton, B. Miller, and J. Sefton, "The deformation of cusps by bonded posterior composite restorations: an in-vitro study," *Br. Dent. J.* **159**, 397–400 (1985).
11. G. J. Pearson and S. M. Hegarty, "Cusp movement of molar teeth with composite filling materials in conventional and modified MOD cavities," *Br. Dent. J.* **166**, 162–165 (1989).
12. A. A. Suliman, D. B. Boyer, and R. S. Lakes, "Cusp movements in premolars resulting from composite polymerization shrinkage," *Dent. Mater.* **9**, 6–10 (1993).
13. N. Meredith and D. J. Setchell, "In vitro measurement of cuspal strain and displacement in composite restored teeth," *J. Dent.* **25**, 331–337 (1997).
14. A. A. Suliman, D. B. Boyer, and R. S. Lakes, "Interferometric measurement of cusp deformation of teeth restored with composite," *J. Dent. Res.* **72**, 1532–1536 (1993).
15. Y. Kinomoto and M. Torii, "Photoelastic analysis of polymerization contraction stresses in resin composite restoratives," *J. Dent.* **26**, 165–171 (1998).
16. C. P. Ernst, G. R. Meyer, K. Klöcker, and B. Willershausen, "Determination of polymerization shrinkage stress by means of a photoelastic investigation," *Dent. Mater.* **20**, 313–321 (2004).
17. H. Ensaff, D. M. O'Doherty, and P. H. Jacobsen, "The influence of the restoration-tooth interface in light cured composite restorations: a finite element analysis," *Biomaterials* **22**, 3097–3103 (2001).
18. A. Versluis, D. Tantbirojn, M. R. Pintado, R. DeLong, and W. H. Douglas, "Residual shrinkage stress distributions in molars after composite restoration," *Dent. Mater.* **20**, 554–564 (2004).
19. P. Hubsch, J. Middleton, and J. Knox, "The influence of cavity shape on the stresses in composite dental restorations: a finite element study," *Comput. Methods Biomech. Biomed. Eng.* **5**, 343–349 (2002).
20. M. Barink, P. C. Van der Mark, W. M. Fennis, R. H. Kuijs, C. M. Kreulen, and N. Verdonschot, "A three dimensional finite element model of the polymerization process in dental restorations," *Biomaterials* **24**, 1427–1435 (2003).
21. J. Jantarat, P. Panitvisai, J. E. A. Palamara, and H. Messerh, "Comparison of methods for measuring cuspal deformation in teeth," *J. Dent.* **29**, 75–82 (2001).
22. A. Wesson, G. R. Goldstein, and A. Schulman, "Flexion characteristics of fixed partial denture frameworks tested by using elapsed-time holographic interferometry," *J. Prosthet. Dent.* **60**, 308–310 (1988).
23. R. J. Van Straten, L. M. Hitge, W. Kalk, and J. Schenk, "A study of acrylic resin denture base material distortion using computer-aided holographic interferometry," *Int. J. Prosthodont* **4**, 577–585 (1991).
24. P. R. Wedendal and H. I. Bjelkhagen, "Dental holographic interferometry in vivo utilizing a ruby laser system I. Introduction and development of methods for precision measurements on the functional dynamics of human teeth and prosthodontic appliances," *Acta Odontol. Scand.* **32**, 131–145 (1974).
25. P. R. Wedendal and H. I. Bjelkhagen, "Dental holographic interferometry in vivo utilizing a ruby laser system. II. Clinical applications," *Acta Odontol. Scand.* **32**, 345–356 (1974).
26. P. R. Wedendal and H. I. Bjelkhagen, "Dynamics of human teeth in function by means of double pulsed holography: an experimental investigation," *Appl. Opt.* **13**, 2481–2485 (1974).
27. D. Fried, R. E. Glena, J. D. B. Featherstone, and W. Seka, "Nature of light scattering in dental enamel and dentin at visible and near-infrared wavelengths," *Appl. Opt.* **34**, 1278–1285 (1995).
28. B. Kahler, A. Kotousov, and K. Borkowski, "Effect of material properties on stresses at the restoration-dentin interface of composite restorations during polymerization," *Dent. Mater.* **22**, 942–947 (2006).
29. N. Verdonshot, W. M. M. Fennis, R. H. Kuijs, J. Stolk, C. M. Kreulen, and N. H. J. Creugers, "Generation of 3-D finite element models of restored human teeth using micro-CT techniques," *Int. J. Prosthodont* **14**, 310–315 (2001).
30. P. Ausiello, A. Apicella, C. L. Davidson, and S. Rengo, "3D-finite element analyses of cusp movements in a human upper premolar, restored with adhesive resin-based composites," *J. Biomech.* **34**, 1269–1277 (2001).
31. P. Ausiello, A. Apicella, and C. L. Davidson, "Effect of adhesive layer properties on stress distribution in composite restorations—a 3D finite element analysis," *Dent. Mater.* **18**, 295–303 (2002).
32. M. Giannini, C. J. Soares, and R. M. de Carvalho, "Ultimate tensile strength of tooth structures," *Dent. Mater.* **20**, 322–329 (2004).
33. P. A. Miguez, P. N. R. Pereira, P. Atsawasuwan, and M. Yamauchi, "Collagen cross-linking and ultimate tensile strength in dentin," *J. Dent. Res.* **83**, 807–810 (2004).
34. E. B. De Las Casas, T. P. M. Cornacchia, P. H. Gouvea, and C. A. Cimini, Jr., "Abfraction and anisotropy-effects of prism orientation on stress distribution," *Comput. Methods Biomech. Biomed. Eng.* **6**, 65–73 (2003).
35. J. R. Zijp, J. J. ten Bosch, and R. A. J. Groenhuis, "HeNe-laser light scattering by human dental enamel," *J. Dent. Res.* **74**, 1891–1898 (1995).
36. R. E. Walton, W. C. Outhwaite, and D. F. Pashley, "Magnification–an interesting optical property of dentin," *J. Dent. Res.* **55**, 630–642 (1976).
37. W. J. O'Brien, "Fraunhofer diffraction of light by human enamel," *J. Dent. Res.* **67**, 484–486 (1988).
38. R. Schilke, J. A. Lisson, O. Bauss, and W. Geurtsen, "Comparison of the number and diameter of dentinal tubules in human and bovine dentine by scanning electron microscopic investigation," *Arch. Oral Biol.* **45**, 355–361 (2000).
39. A. A. Suliman, D. B. Boyer, and R. S. Lakes, "Polymerization shrinkage of composite resins: comparison with tooth deformation," *J. Prosthet. Dent.* **71**, 7–12 (1994).